A numerical investigation on NO2 formation reaction pathway in a natural gas–diesel dual fuel engine

Li, Yu; Li, Hailin; Guo, Hongsheng

Publisher's version / Version de l'éditeur:
https://doi.org/10.1016/j.combustflame.2017.12.006
Combustion and Flame, 190, pp. 337-348, 2017-12-27

A Numerical Investigation on NO_2 Formation Reaction Pathway in a Natural Gas-Diesel Dual Fuel Engine

Yu Li and Hailin Li

West Virginia University

Hongsheng Guo

National Research Council Canada

Abstract

This paper numerically investigated the NO_2 formation pathway in a natural gas (NG)-diesel dual fuel engine using a computational fluids dynamics (CFD) model CONVERGE. The fuel chemistry coupled was a reduced primary reference fuel (PRF) mechanism consisting of 45 species and 142 reactions including the NO_x mechanism from GRI chemistry. The NO_2 formation pathway was investigated by examining the rate of production (ROP) of key species dominating NO_2 formation in each cell. The ROP of the key species was further processed to derive the representative creation reactions (RCR) of NO_2 (RCR_{NO2}). The simulation revealed that the NO_2 produced during main combustion stage was formed in the hot combustion products of n-heptane spray through reaction pathway C_7H_{15}->CH_2O->HCO->H->O->NO_2 and the interface between the hot combustion products and NG-air mixture dominated by the HO_2 produced through reaction pathway CH_4->CH_3->CH_2O->HCO->HO_2. The NO_2 formed in hot combustion products during main combustion stage was later on destructed to NO and was not able to survive through the expansion process. In comparison, the NO_2 formed during the post combustion expansion process was dominated by HO_2 radical formed in the interface between the NO-containing combustion products and unburned NG-air mixture. It was concluded that the increased conversion from NO to NO_2 in a NG-diesel dual fuel engine was due to the increased HO_2 produced through the reaction path: CH_4->CH_3->CH_2O->HCO->HO_2 in the post combustion stage. The availability of methane necessary for the production of HO_2 after the completion of the main combustion process was the main factor contributing to the significantly increased NO_2 emissions from NG-diesel dual fuel engines. The research aiming at reducing NO_2 emissions from dual fuel engines should focus on the approaches capable of significantly improving the combustion efficiency of NG.

Keywords: NO_2 formation pathway, NG-diesel dual fuel engine, CFD, chemical kinetics process.

Nomenclature

3-D: Three dimensional

ATDC: After top dead center

bmep: Brake mean effective pressure

CFD: Computational fluids dynamics

CI: Compression ignition

ISDP: Instantaneous species destruction pathway;

NG: Natural gas

NO: Nitric oxide

NO_2: Nitrogen dioxide

NO_x: Nitrogen oxides

PRF: Primary reference fuel

RCR: Representative creation reaction

RDR: Representative destruction reaction

ROP: Rate of production

Introduction

The nitrogen oxides (NO_x) emitted from diesel engines consists of nitric oxide (NO) and nitrogen dioxide (NO_2). Although NO_2 has been reported by Boezen, et al. [1] as a respiratory irritant to human health, especially to children with bronchial hyper-reactivity, the study of NO_2 emissions from diesel engines is limited because NO_2 emissions account for only a very small proportion of NO_x emissions, especially at medium to high load.

Dual fuel engines are attracting more attention in recent years for their fuel flexibility and high thermal efficiency in burning gaseous fuels in compression ignition (CI) engines [2]. The recent research on NOx emissions from natural gas (NG)-diesel dual fuel engines reported a significant impact of the addition of NG to intake mixture on NO_2 emissions, especially at low load [3]. For example, Liu et al. [3] experimentally investigated the NO_2 emissions from a heavy-duty diesel engine fumigated with NG or hydrogen (H_2). The NO_2 emissions from diesel engine were affected by the load of engine operation. For example, the NO_2/NO_x ratio was found to vary from 5% (70% load) to 15% (10% load). The addition of NG to diesel engine significantly increased NO_2 emissions and NO_2/NO_x ratio. The maximum NO_2 emissions from the dual fuel engine were about three (at 70% load) to five (at 10% load) times of those observed with diesel only operation [3]. A similar phenomenon has been reported with the addition of H_2 [3-8]. The presence of the premixed fuel in a CI engine featuring diffusion combustion may enhance the formation of NO_2 in a dual fuel engine. Although numerous researches reported the significant impact of premixed gaseous and liquid fuels on NO_2 emissions from CI dual fuel engines, the research on the fundamental knowledge of the NO_2 formation reaction pathway in dual fuel engines has not been reported. The development of approaches aiming to control NO_2 emissions from dual fuel engines requests the detailed investigation of the NO_2 formation reaction pathway.

Previous fundamental research on NO_x formation has investigated the formation of NO at high temperature and its conversion to NO_2 promoted by hydrocarbons [9-12]. For example, NO_2 can be produced through the reaction NO + RO_2->NO_2 + RO, where R=H, CH_3, C_2H_5, ...C_nH_{2n+1} [9]. In the past decades, the NO_2 formation mechanism was further revealed by examining the NO–NO_2 conversion reaction: NO+HO_2->NO_2+OH. For example, Hori et al. [10] numerically and experimentally examined the factors affecting the NO–NO_2 conversion including hydrocarbon type, residence time, and reaction temperature. It was concluded that the NO-NO_2 conversion was only observed at a relatively low temperature range from 650 to 1000K. Such a conversion was dominated by the capability of hydrocarbons in producing reactive radicals such as OH and O. Mueller, et al. [11] experimentally and numerically studied the NO to NO_2 conversion in a flow reactor at a low-temperature range (750-1100K). The NO to NO_2 conversion was affected by the pressure and stoichiometry of the air/fuel mixture. Kyne, et al. [12] studied the NO to NO_2 conversion in counterflow diffusion flames. The examination of the rate of production (ROP) and sensitivity analysis indicated that the NO to NO_2 conversion was more sensitive to the concentrations of CO_2, CO, hydrocarbons, NO and NO_2 than to the initial pressure. However, little fundamental research on the NO_2 reacxtion pathway in NG-diesel dual fuel engines has been reported.

NG-diesel dual fuel engines have the feature of diffusion combustion [2,3,4]. The investigation on NO_2 formation reaction pathway in NG-diesel dual fuel engines requests the examination of the spatial distributions of the

temperature, pressure and volumetric concentrations of key species involved in the formation of NO_2, which are difficult to measure but can be made avaliable through numerical simulation using the computational fluid dynamics (CFD) model. With the known temperature, pressure and volumeric concentrations of key species, the reaction rate of each reaction and ROP of each species can be calculated. The analysis of the reaction rates of key reactions and ROPs of key species involved in NO_2 formation can lead to the development of a NO_2 formation reaction pathway including the key species and series of reactions dominating NO_2 formation in dual fuel engines.

This research investigates the NO_2 formation reaction pathway in a NG-diesel dual fuel engine using the commercial software CONVERGE [13]. A reduced primary reference fuel (PRF) mechanism is coupled to the SAGE chemistry solver to calculate the chemical reactions occurring in the combustion chamber [14]. The model is first validated against cylinder pressure, heat release rate, NO_x emissions, and NO_2/NO_x ratio over a wide range of substitution ratios when the engine was operated at constant load. The validated model was applied to simulate the combustion process and derive the pressure, temperature and concentration of each species in each cell. These data are further processed using an in-house post-processing tool [15] to calculate the instantaneous ROP data using CHEMKIN [16] with species and thermal data imported from the CONVERGE-SAGE model. A representative creation reaction (RCR) method was applied to analyze the chemical kinetics process of the NO_2 formation mechanism. The analysis of the simulation data will focus on: (1) the spatial distributions of NO, NO_2, equivalence ratio (phi), temperature, and methane; (2) The key species and the key reactions dominating the formation of NO_2 and consumption of these species; (3) the key reaction pathways leading to NO_2 formation in dual fuel engines and the competition among these key pathways in producing NO_2 in different region in the bulk gas; (4) the impact of substitution ratio on the NO_2 formation in dual fuel engines.

Engine Operation Condition, Numerical Simulation Model and ROP Evaluation Method

Engine Specification and Operating Condition

The experiments were conducted in a single-cylinder version of Caterpillar's 3400-series diesel engine with a compression ratio of 16.25, bore of 137.2 mm, and stroke of 165.1mm. The engine was converted to operate on NG-diesel dual fuel combustion mode with NG injected into the intake air using a port fuel injector. The diesel fuel was directly injected into the cylinder using a common-rail fuel system at fuel pressure of 525 bar. The diesel injection timing was fixed at $-7°\ CA$ after the top dead center (ATDC). No EGR was applied in the experiments. More details of the test engine and operating conditions can be found in the literature [17].

In this research, the simulated engine was operated at 910 rpm and 4.05 bar brake mean effective pressure (bmep). The constant load operation was achieved by reducing the diesel fuel injected with the addition of NG. As illustrated in Table 1, the contribution of NG to total energy was varied from 0 to 75% with the addition of 0% to 4.21% NG into intake air. The energy substitution ratio of NG is defined as:

$$\alpha_{NG} = \frac{m_{NG} LHV_{NG}}{m_{NG} LHV_{NG} + m_{diesel} LHV_{diesel}} \qquad (1)$$

where α is the substitution ratio, m is the mass flow rate, LHV is the low heating value.

Table 1 The mass of diesel and natural gas injected (mixed) during each engine cycle [19].

Cases		Diesel fuel, mg/cycle	Natural Gas		
			Mass, mg/cycle	Vol. cons. in intake mixture	NG contribution to fuel energy
Case A	0 NG	66.2	0.0	0.0	0%
Case B	25 NG	49.7	15.5	1.33%	25%
Case C	50 NG	34.8	32.2	2.72%	50%
Case D	75 NG	18.1	50.9	4.21%	75%

Simulation Model

The numerical simulation work was conducted using the commercial software CONVERGE-SAGE model. The diesel fuel was represented by n-heptane. NG was represented by methane. The physical property of diesel fuel was represented by tetradecane ($C_{14}H_{30}$) to simulate the spray development, atomization, vaporization and the mixing of n-heptane with air. The detailed description of the model can be found in the literature [15]. The fuel chemistry used in this study is a reduced PRF mechanism proposed by Ra et al. [14], which consists of 41 species and 130 reactions. The NOx mechanism (4 species and 12 reactions) from GRI chemistry [18] is added for the simulation of NOx. Table 2 shows the important reactions involved in the production and consumption of NO_2.

Table. 2 Key reactions discussed in this study.

R1	$HO_2+NO=NO_2+OH$	R8	$C_3H_6=C_2H_3+CH_3$	R15	$CH_2+O_2=CH2O+O$
R2	$O+NO+M=NO_2+M$	R9	$C_3H_6+O=CH_2CO+CH_3+H$	R16	$CH_2O+OH=H_2O+HCO$
R3	$NO_2+O=NO+O_2$	R10	$C_2H_3+O_2=CH_2O+HCO$	R17	$HCO+M=CO+H+M$
R4	$H+NO_2=NO+OH$	R11	$CH_3+O_2=CH_2O+OH$	R18	$H+O_2=O+OH$
R5	$C_7H_{15}=C_2H_5+C_2H_4+C_3H_6$	R12	$CH_3+OH=CH_2+H_2O$	R19	$CH_4+OH=CH_3+H_2O$
R6	$C_7H_{15}+O_2=C_7H_{15}O_2$	R13	$CH_2CO(+M) =CH_2+CO (+M)$	R20	$H+O_2 (+M) =HO_2 (+M)$
R7	$C_2H_4+OH=CH_2O+CH_3$	R14	$CH_3+O=CH_2O+H$	R21	$HCO+O_2=CO+HO_2$

The model was validated against cylinder pressure, heat release rate, and the emissions of methane, and CO obtained from a dual fuel engine over a wide range of energy substitution ratios by NG (0-75%). The detailed validation of fuel chemistry and emissions can be found in the literature [15, 19]. This model can also be applied to simulate the NO and NO_2 emissions from a NG-diesel dual fuel engine. Fig. 1 compares the simulated and measured variations of indicate specific emissions of NO_2, NO, NOx, and the NO_2/NOx molar ratio with changes in NG substitution ratio. For computational purpose, NO, NO_2, and NOx are presented in this paper as equivalent NO by mass. It was found that the CFD model could predict the qualitative variation trends of both NOx and NO_2 emissions as well as the NO_2/NOx ratio for different NG substitution ratios, suggesting that the model can be applied to investigate the NO_2 formation reaction pathway in the NG-diesel dual fuel engine.

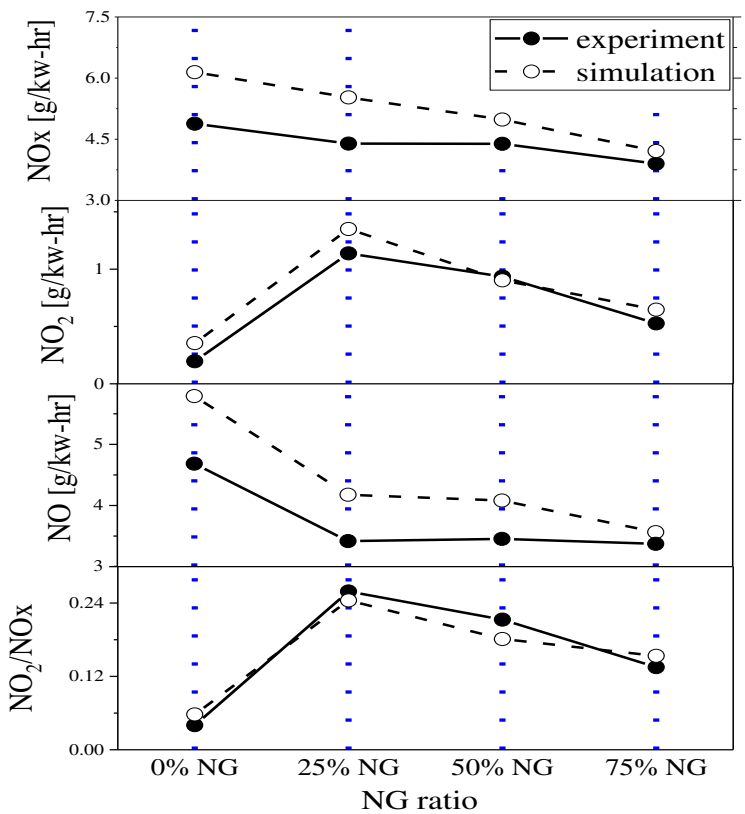

Fig. 1 Comparison of simulated NO_x, NO_2, NO emission and NO_2/NO_x mass ratio with experimental data.

Calculation of ROP of the Key Species

The temperature, pressure, and species concentrations at each computational cell calculated using the CFD model are exported to a 'column format' file by CONVERGE [13]. A MATLAB code was developed to read the temperature, pressure and species concentrations in 'column format' file. The ROP of each species in each cell was calculated using CHEMKIN. The calculated ROP data were analyzed and visualized by an in-house MATLAB code. Fig. 2 shows the flowchart of the CONVERGE-SAGE model and ROP calculation. The detailed description of the post-processing method and ROP evaluation method can be found in [15].

Representative Creation/Destruction Reaction

Among all the reactions involved in the ith species creation in each computational cell, there exists a reaction that has the largest production. Such a reaction has the largest contribution to the creation of the ith species and is defined as the RCR of the ith species. Similarly, the reaction that has the largest contribution to the destruction of the ith species is defined as the representative destruction reaction (RDR) of the ith species. This research will examine the RCR dominating the formation of NO_2 noted as RCR_{NO2} in NG-diesel dual fuel engines. The examination of the NO_2 formation mechanism will be conducted by examining the formation of radicals such as H, OH, and HO_2 through the destruction of other species originating from CH_4 and n-Heptane. The analysis of the RDR of these species helps to derive the NO_2 formation reaction pathway.

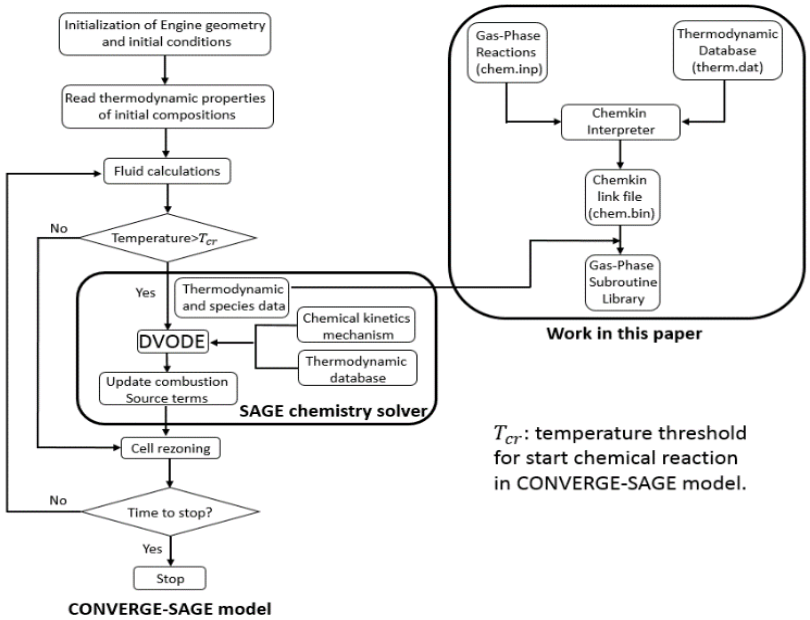

Fig. 2 Flow chart for the CONVERGE-SAGE model and ROP calculation [15]

Instantaneous Species Destruction Pathway

In this research, the instantaneous species destruction pathway (ISDP) analysis was conducted by examining the instantaneous contribution of each reaction to the destruction of each species using equation (2).

$$\beta_{d,i,j} = \frac{\omega_{d,i,j}}{\omega_{d,i}} \qquad (2)$$

where $\omega_{d,i,j}$ represents the destruction rate of $the\ i^{th}$species by $the\ j^{th}$reaction, $\omega_{d,i}$ is the destruction rate of the ith species, which is calculated by $\sum \omega_{d,i,j}$, and $\beta_{d,i,j}$ is the normalized contribution of the jth reaction to i^{th} species destruction.

In this study, the ISDP analysis was performed in the RCR_{NO2}-O and RCR_{NO2}-HO_2 regions during the main combustion stage and post combustion expansion processes to identify the main reaction pathway and key species dominating the consumption of species leading to the formation of NO_2 in NG-diesel dual fuel engines. The main combustion stage is defined as the period from CA10 to CA90. The heat release observed after CA90 in this dual fuel engine is released through burning of NG survived the main combustion process as diesel has been completely consumed. The NO_2 produced after CA90 is considered as NO_2 formed during post combustion expansion process.

Calculation of Equivalence Ratio

The equivalence ratio (Phi) at each computational cell is calculated using equation (3) [13],

$$Phi = \frac{2\sum N_i \eta_{C,i} + 0.5\sum_i N_i \eta_{H,i}}{\sum N_i \eta_{O,i}} \qquad (3)$$

where N_i is the number of moles of the ith species in each cell, $\eta_{C,i}, \eta_{H,i}, \eta_{O,i}$ are the number of carbon (C), hydrogen (H) and oxygen (O) atoms in each species, respectively. In this paper, the elements in H_2O and CO_2 are not considered in equivalence ratio calculation.

Results and Discussion

Fig. 3 shows the effect of the NG substitution on the variations of the total mass and production rate of NO_2, and heat release rate with change in crank angle. The NO_2 mass production rate is the derivative of the total NO_2 mass with respect to crank angle, i.e. $dm_{NO2}/d\theta$, where m_{NO2} is the total mass of NO_2 in cylinder. The significant variation in $dm_{NO2}/d\theta$ before $10\ °CA\ ATDC$ suggests the competition among reactions that create/destruct NO_2 during main combustion stage. The addition of NG was found to significantly reduce the NO_2 formation at the early combustion stage. The NO_2 observed at diesel only operation mode (0NG) is mainly produced during the combustion process with the peak NO_2 production observed before $10°\ CA\ ATDC$. The addition of 25NG, 50NG and 75NG elongated the period of NO_2 production beyond the completion of combustion, continued into the late expansion process and even into the exhaust valve open (EVO). The peak NO_2 production rate was retarded to around 30, 50 and $100°\ CA\ ATDC$ for the cases of 25NG, 50NG, and 75NG, respectively. It is evident that most of the NO_2 is produced during the post combustion process in a dual fuel engine. This research will first examine the NO_2 formation reaction pathway in a NG-diesel dual fuel engine using the 25NG case as an example. The impact of the increased NG addition on NO_2 formation will be examined and discussed.

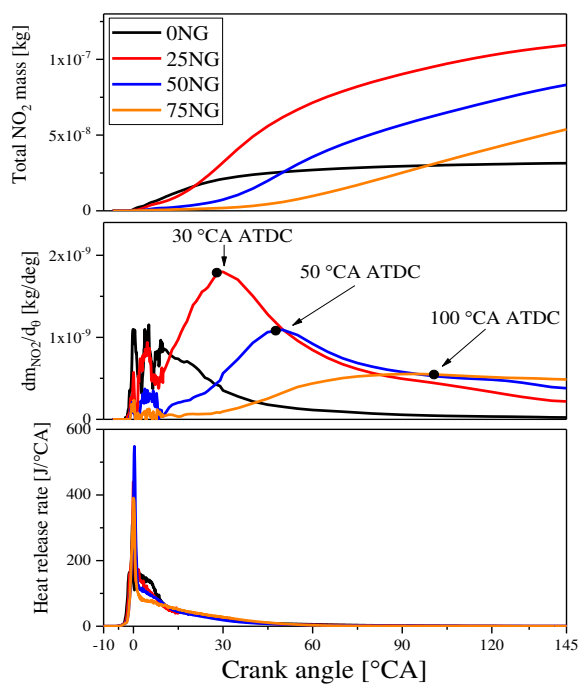

Fig. 3 Effect of diesel substitution by NG on the simulated variation of total NO_2 mass, total NO_2 production, and heat release rate with change in crank angle.

In this study, the regions of the bulk gas with positive and negative net NO_2 production rates are defined as Region 1 and Region 2, respectively. Fig. 4 shows the variations of the total NO_2 mass in Region 1 and Region 2 with changes in crank angle for 0NG and 25NG case, respectively. The total mass of NO_2 in Region 1 is much higher than that in Region 2, indicating that the NO_2 in the region having net NO_2 consumption (Region 2) can be ignored. The NO_2

formation mechanism in NG-diesel dual fuel engines can be explained by analyzing NO_2 production in Region1 due to relatively less NO_2 in Region 2.

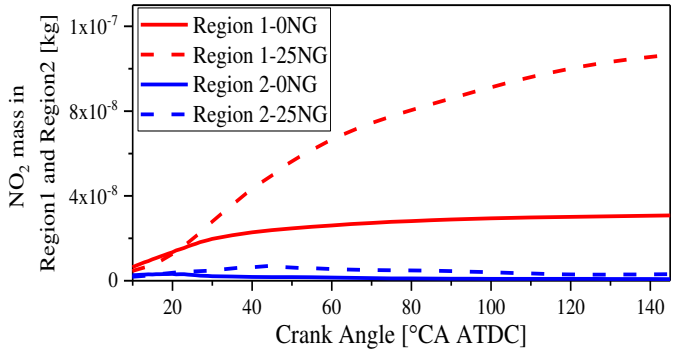

Fig. 4 Variation of the total NO_2 mass in Region1 and Region2 with change in crank angle for diesel and 25NG, respectively. Red line: Region1, blue line: Region2.

For the 25NG case, the NO_2 formation mechanism during the main combustion stage and post combustion expansion process was examined at CA50 ($7°\ CA\ ATDC$) and CA95 ($60°\ CA\ ATDC$), respectively. Therefore, this section includes three sub-sections. In the 1st sub-section, the NO_2 formation nature during main combustion stage is studied. In the 2nd subsection, the NO_2 formation nature at post combustion stage is studied. In the 3rd subsection, the effect of NG substitution ratio on NO_2 formation at 25NG, 50NG and 75 NG during post combustion expansion process is compared.

NO_2 Formation during Main Combustion Stage

Fig. 5 shows the distributions of NO, NO_2, CH_4, HO_2, O, temperature, RCR_{NO2} and NO_2 production rate in the bulk gas as well as the phi-T diagram observed at CA50 noted as 7 °CATDC for the case of 25NG. It is found that NO is mainly distributed within the high temperature region indicating the formation of NO in high temperature combustion products of diesel, which is consistent with the NO formation characteristics reported in the literature [20, 21]. In comparison, NO_2 is mainly distributed in the interface area between the hot region containing most NO and relatively cool region containing the unburned NG-air mixture as indicated by the distribution of unburnt methane. The NO_2 production is determined by reactions R1 and R2 which involve HO_2 and O, respectively. In this research, the in-cylinder region where the production of NO_2 is dominated by R1 involving HO_2 is defined as the RCR_{NO2}-HO_2 region, while the region where the production of NO_2 is dominated by R2 with O involved is defined as the RCR_{NO2}-O region. Both the RCR_{NO2}-O and RCR_{NO2}-HO_2 regions are featured with low local equivalence ratios, indicating that the formation of NO_2 mainly occurs in lean mixtures located at the edge of diesel spray plume. Such a lean mixture can be either the unburned methane-air mixture featured with low temperature or the mixture of n-heptane, methane and air located in the edge of n-heptane spray plume. The local temperature in RCR_{NO2}-O region is over 1600K as shown in phi-T diagram, indicating the formation of NO_2 through R2 in the high temperature region. In comparison, the temperature of the RCR_{NO2}-HO_2 region (1000 to 1700 K) is much lower than that of the RCR_{NO2}-O region. As shown in Figure 6, the highest NO_2 molar fraction is observed at the interface between hot

combustion products containing a high concentration of NO and the relatively cool region containing the methane/air mixture, which is accompanied with high molar fraction of HO_2. This indicates that the NO_2 observed at 7 °CA ATDC is mainly formed in the RCR_{NO2}-HO_2 region. The NO_2 production rate in RDR_{NO2}-O region is significantly higher than that in RDR-HO_2 region. This is due to the high local temperature in RDR_{NO2}-O region that promote the production of O radical by R18.

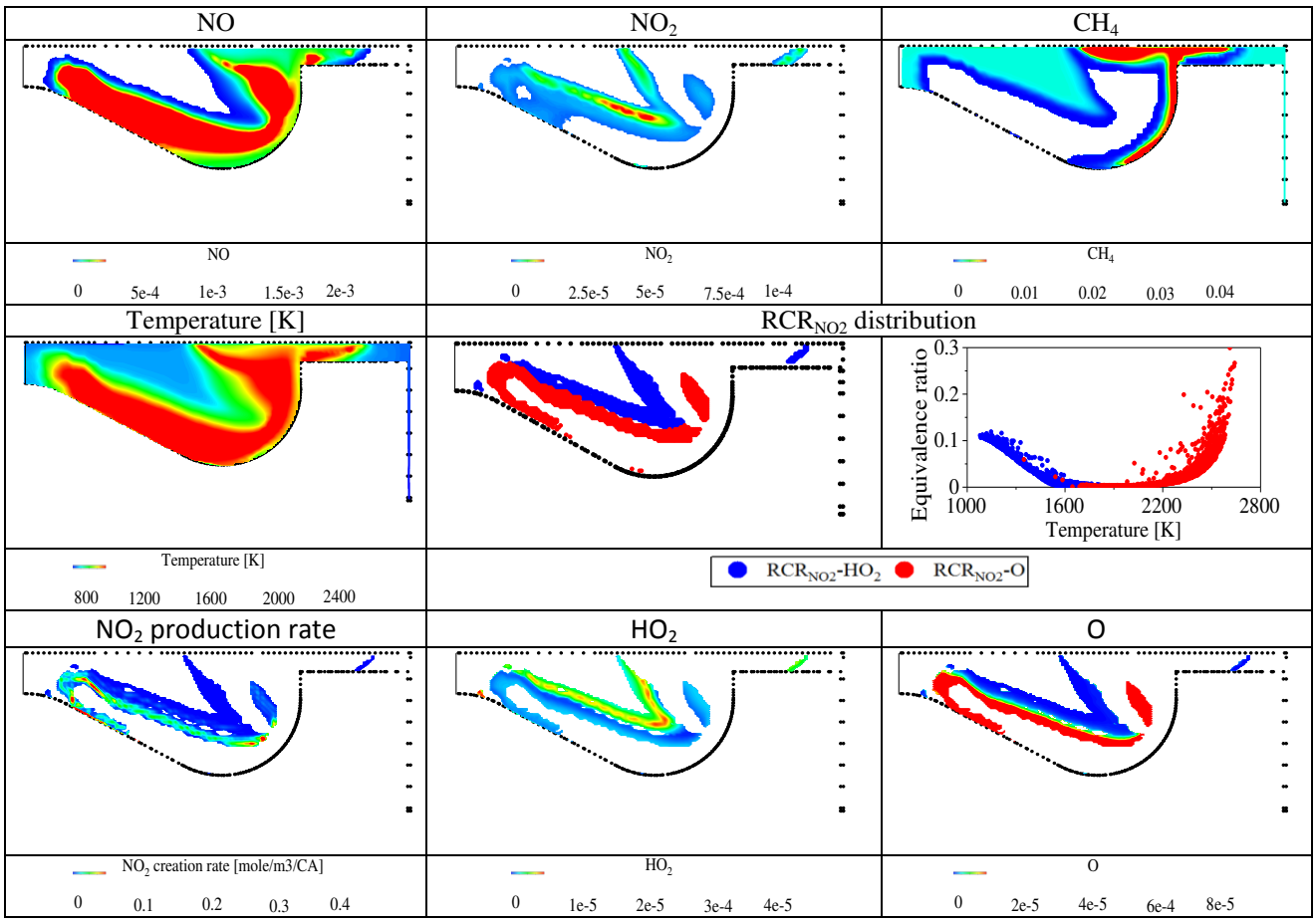

Fig. 5 Temperature, RCR_{NO2} distribution in cut-plane and phi-T diagram, CH_4, NO, NO_2, HO_2, and O molar fraction, NO_2 production rate at Region1, CA50, 7° $CA\ ATDC$, 25NG case.

The formation reaction pathway of NO_2 in the RCR_{NO2}-HO_2 and RCR_{NO2}-O region at 7 °CA ATDC is investigated using the ISDP method. As shown in Fig. 6, the instantaneous species destruction pathway in the RCR_{NO2}-O region and RCR_{NO2}-HO_2 region are significantly different. For the RCR_{NO2}-O region, the heptyl radical consumption is dominated by decomposition via R5 instead of oxygen addition via R6, which is well known for low-temperature combustion. The products of R5, such as C_2H_4, C_2H_5, and C_3H_6, in turn produce the formaldehyde radical (CH_2O) through a complex destruction pathway, leading to the production of a large amount of H and O radical by the reaction route R16- R17-R18. The H and O radicals not only take part in NO_2 formation through R2 but also NO_2 consumption through R3 and R4. Meanwhile, the reactions R9, R14 and R15 are involved in O/H radical production/consumption, which may also promote the chain branching reaction in the RCR_{NO2}-O region.

Accordingly, the H and O radicals dominating the formation of NO_2 in the RCR_{NO2}-O region are produced through reaction pathway: C_7H_{15}->CH_2O->HCO->H->O. In comparison, the formation of NO_2 in the RCR_{NO2}-HO_2 region is dominated by the HO_2 produced through reaction pathway CH_4->CH_3->CH_2O->HCO->HO_2. The HO_2 present in the RCR_{NO2}-HO_2 region is produced through co-oxidation between lean mixture consists of unburned methane and diesel spray periphery. The examination of the reaction path way identified HCO as the key species dominating the formation of the key radicals such as H and O in the RCR_{NO2}-O region, and HO_2 in the RCR_{NO2}-HO_2 region. The HCO produced in the RCR_{NO2}-O and RCR_{NO2}-HO_2 regions can be theoretically traced back to the dissociation of diesel and CH_4, respectively.

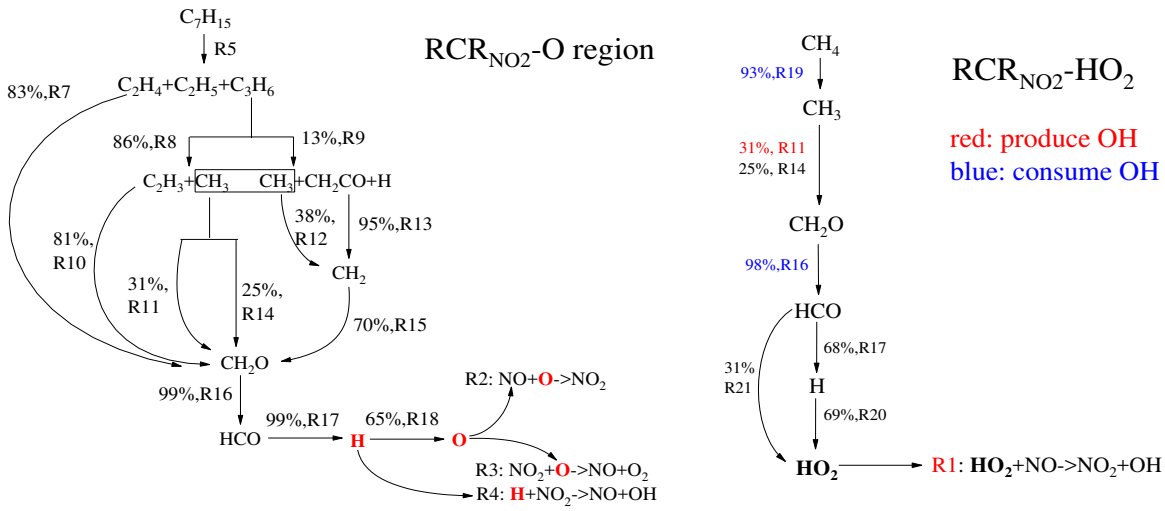

(a) RCR_{NO2}-O Region (b) RCR_{NO2}-HO_2 Region

Fig. 6 Contribution of reaction to species destruction for the RCR_{NO2}-O and RCR_{NO2}-HO_2 regions at $7°\ CA\ ATDC$, 25NG case.

As shown in Fig. 6 (b) and Table 2, the reactions R11, R20, and R21 in RCR_{NO2}-HO_2 region involves O_2, which suggests the importance of oxygen for HO_2 production and the NO conversion to NO_2. This is consistent with the phi-T distribution of the RCR_{NO2}-HO_2 region shown in Fig. 5, where the low local equivalence ratio indicates the availability of O_2. The reactions marked with red and blue in Fig. 6 (b) represents production and consumption of OH radical, respectively. The OH produced by R1 may take part in R16 and R19, which promote the chain branching reaction in the RCR_{NO2}-HO_2 region. The production and consumption of HCO and H radicals prior to the formation of O and HO_2 exist in both RCR_{NO2}-O region and RCR_{NO2}-HO_2 region. The consumption of HCO in the RCR_{NO2}-O region is dominated by R17 (99%). In comparison, the HCO production in the RCR_{NO2}-HO_2 region is dominated by R17 (68%) and R21 (31%). The consumption of H is dominated by R18 (65%) in the RCR_{NO2}-O region and by R20 (69%) in the RCR_{NO2}-HO_2 region, respectively. This suggests that the reaction pathway of NO_2 formation and consumption in the RCR_{NO2}-O and RCR_{NO2}-HO_2 regions are dominated by the competition among these reactions.

Fig. 7 compares the effect of temperature on the forward reaction rate constants of R17 and R21, R18 and R20, respectively. The forward reaction rate constant of R17 is lower than that of R21 when the local temperature is below 1625K. However, the reaction rate constant of R17 increases significantly with the increasing temperature, especially when the local temperature is over 1625K. The reaction rate constant of R18 increases exponentially with temperature, and is lower than that of R20 when the local temperature is low (<1100K). This helps to explain the different HCO consumption pathways in the RCR_{NO2}-HO_2 and RCR_{NO2}-O regions shown in Fig. 6. As shown in the phi-T diagram in Fig. 5, the temperature of the RCR_{NO2}-HO_2 region is lower than that of the RCR_{NO2}-O region. This makes R17 dominate HCO consumption (99%) in the RCR_{NO2}-O region featuring with high temperature. The consumption of HCO through R21 in the RCR_{NO2}-O region is negligible. In comparison, the HCO in RCR_{NO2}-HO_2 is consumed through R17 for the production of H and R21 for the production of the HO_2 radical. In comparison, R18 and R20 dominate the H consumption in the RCR_{NO2}-O and RCR_{NO2}-HO_2 regions, respectively, due to the significantly high and low reaction rate constants. The H produced in RCR_{NO2}-O through R17 can either convert NO_2 to NO through R4, or produce O through R18 which can either convert NO_2 to NO through R3 or convert NO to NO_2 through R2. The consumption of H produced in RCR_{NO2}-HO_2 produces HO_2 through R20, which promotes the conversion from NO to NO_2 through R1. In summary, the consumption of HCO in the RCR_{NO2}-HO_2 region produces HO_2 through R17-R20, and R21, and enhances the conversion from NO to NO_2 through R1. In comparison, the ~~the~~ consumption of HCO in the RCR_{NO2}-O region produces H radical and O radicals, which enhances the conversion from NO_2 to NO through R3 and R4, as well as the conversion from NO to NO_2 through R2.

The local temperature is the key factor that dominates the reaction pathway shown in Fig. 6. The CH_4 concentration in the RCR_{NO2}-HO_2 region is significantly higher than that in the RCR_{NO2}-O region, leading to the HO_2 production dominated by CH_4->CH_3->CH_2O->HCO->HO_2. It is also observed in Fig. 7 that increasing local temperature will increase the O and H production in the RCR_{NO2}-O region and enhance NO_2 destruction to NO by reaction R3 and R4. Thus, the NO_2 net production rate in the RDR-O region is dominated by the intense competition among R2, R3 and R4. Therefore, although a significantly high temperature and O radical concentration is observed in RDR_{NO2}-O region, the NO_2 produced by R2 due to high temperature and O radical concentration may be consumed by reverse reaction of R3 and R4. This explains the higher net NO_2 production rate but a lower NO_2 concentration observed in RCR_{NO2}-O region, as shown in Fig. 5. However, the low temperature in the RCR_{NO2}-HO_2 region inhibits the production of O and H radicals and the destruction of NO_2 to NO. This explains the formation and high concentration NO_2 at the intersection of the NO and CH_4/air mixture due to the high rate of formation and low destruction rates at low temperature. As a result, the NO_2 produced in the main combustion stage of a NG-diesel dual fuel engine is mainly formed in the RCR_{NO2}-HO_2 region. In comparison, the NO_2 formed in the hot combustion products during the main combustion stage was later on reduced to NO.

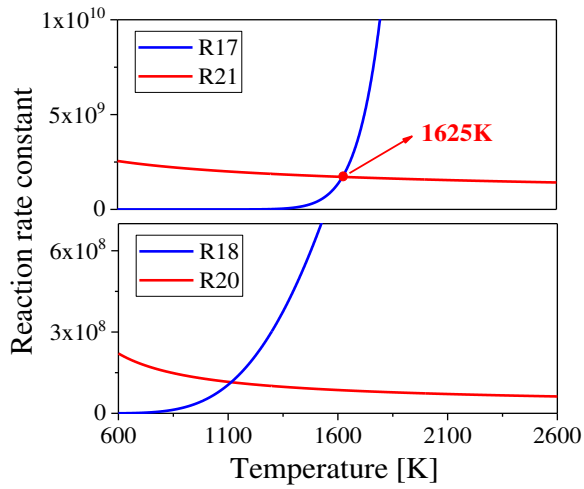

Fig. 7 Effect of temperature on the forward reaction rate constant of R17, R21, and R18, R20.

NO_2 Formation in Post Combustion Stage

Fig. 8 shows the distributions of temperature, RCR_{NO2} region, NO_2 production and mole fractions of CH_4, NO, NO_2 simulated for the 25NG case at CA95 (60 °CA ATDC). Negligible NO_2 can be observed in the high temperature zone representing the combustion products of diesel, indicating the complete destruction of NO_2 formed in the hot combustion production zone during the main combustion stage. It is highly likely that NO_2 that survived to the exhaust valve opening (EVO) is formed in RCR_{NO2}-HO_2, especially during the post combustion stage. Similar to the NO_2 distribution at main combustion stage (7°CA ATDC), the high NO_2 concentration and NO_2 production is observed at the interface between the cool CH_4/air mixture and high hot combustion products containing NO. As marked in Fig. 8, there are three regions ((1)-(3) shown in Figure 8) featuring high NO_2 concentrations and high NO_2 production rate. They are all located in the RCR_{NO2}-HO_2 region. Thus, it is evident that the NO_2 produced during post combustion process is mainly formed in the RCR_{NO2}-HO_2 region. There is insignificant amounts of NO and NO_2 observed in the region featuring low temperature and high methane concentration (marked as (4) in Fig. 8). Such a region is recognized as a "dead" one which does not participate in active chemical reactions, does not have a chance to mix with hot combustion products but provides the main source of unburned methane [3, 19].

Fig. 9 shows the instantaneous contribution of the main reactions to the destruction of species involved in the RCR_{NO2}-HO_2 region at 60 °CA ATDC. The HO_2 needed for NO conversion to NO_2 is produced by the reaction pathway: CH_4->CH_3->CH_2O->HCO->HO_2, which is similar to that observed in the RCR_{NO2}-HO_2 region at 7 °CA ATDC shown in Fig. 6. Compared with Fig.6b, the notable difference observed in Fig. 9 is the more important contribution of R21 to the consumption of HCO radical. This is due to the decreased temperature during expansion process, which may make the reaction rate constant of R21 more pronounced.

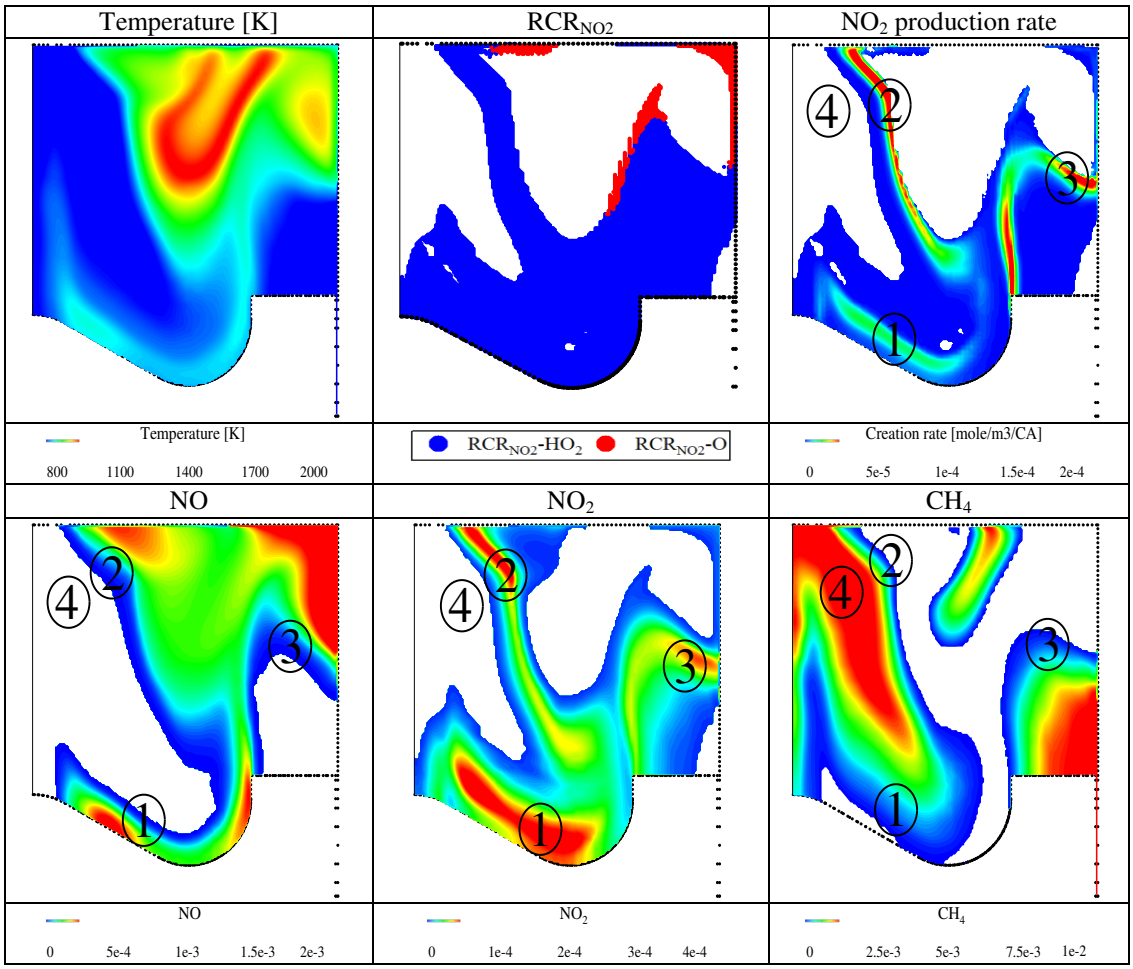

Fig. 8 The temperature, RCR$_{NO2}$ distribution, NO_2 production, CH_4, NO, NO_2 molar fraction simulated at Region1, 60 °CA ATDC, 25NG case.

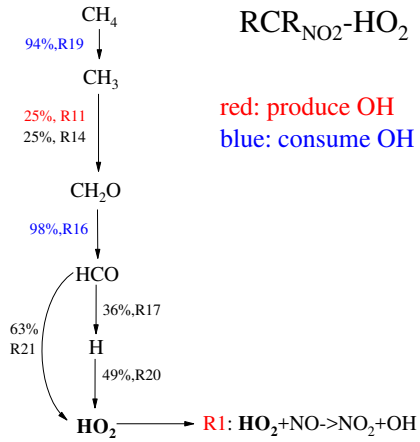

Fig. 9 Contribution of reaction to species destruction for the RCR$_{NO2}$-HO_2 region at 60 °CA ATDC, 25NG case.

Analysis of Fig. 5 and Fig. 8 reveals the difference of NO_2 formation nature in dual fuel engine during main combustion stage and post combustion expansion stage. As discussed before, the HO_2 radical needed for NO conversion to NO_2 in the RCR_{NO2}-HO_2 region is produced via the reaction pathway: CH_4->CH_3->CH_2O->HCO->HO_2. The unique combustion characteristics of NG-diesel dual fuel engines makes the methane necessary for the production of HO_2 still available after the completion of the main combustion process [19]. The mixing of the unburned NG-air mixture with hot combustion products increases the temperature, and initiates the low temperature oxidation reaction of methane which leads to HO_2 production during the post combustion stage. The HO_2 produced enhances the conversion of NO to NO_2 at the interface between the hot NO containing combustion products and cool NG-air mixture. The NO_2 formed in the RCR_{NO2}-HO_2 region during the late main combustion and post combustion expansion process will survive until EVO and exit the engine as NO_2 emissions. In comparison, for a traditional diesel engine, there is neither premixed methane nor available unburned diesel fuel (n-heptane in this simulation) to produce HO_2 after the completion of the combustion process as the diesel was almost completely burned in diesel engine. Therefore, the NO_2 emissions from a diesel engine are mainly formed during the main combustion process. This explains the formation of more NO_2 in NG-diesel dual fuel engines than in traditional diesel engines, as shown in Fig. 1 and Fig. 3.

Effect of NG Substitution Ratio on NO_2 Formation

As shown in Fig. 1, the substitution of diesel by NG significantly increased NO_2 emissions with the maximum NO_2 emission observed at 25NG among the 4 cases examined. Further increasing the substitution ratio from 25% to 75% decreased the emissions of NO_2. As previously discussed, the NO_2 emissions from NG-diesel dual fuel engines is mainly formed in the RCR_{NO2}-HO_2 region through CH_4->CH_3->CH_2O->HCO->HO_2. Thus, this observation can be further elaborated by examining the volume of the RCR_{NO2}-HO_2 region and the average reaction rate of R1 in this region.

A detailed analysis of the NG substitution effect on diesel spray volumetric ratio, hot combustion products and velocity field was presented in a recent study [19]. In order to understand the effect of NG substitution ratio on NO_2 emission in this research, the findings in the previous study need to be recounted. As presented in reference [19], the diesel was continuously injected when the spray tip reached the piston. The hot combustion product bounced back toward the centerline of combustion chamber. This suggests that more momentum of the hot combustion products can be made available when more diesel was injected. As a result, velocity field of the hot NO-containing regions becomes stronger and its volume becomes larger when more diesel fuel is injected.

With the engine speed and load of the four computational cases kept as constant, increasing the NG substitution ratio decreases the mass of diesel injected in each cycle as shown in Table 1. The decreased mass of diesel injected may reduce the volume of the diesel injection plume and combustion products of diesel. This may decrease the NO produced within the diesel spray during the combustion process, and the volume of interface between the hot combustion products and the cool unburned NG-air mixture, and reaction rates of chemical reactions occurring within this region. This is supported by examining the volume of the RCR_{NO2}-HO_2 region and comparing the RCR_{NO2}-HO_2 distribution observed at different NG substitution ratio. Fig. 10 and Fig. 11 shows the distributions of

temperature, RCR_{NO2} region, NO_2 production rate and mole fractions of CH_4, NO, NO_2 simulated for the 50NG and 75NG case at 60 °CA ATDC. Several common features can be observed by comparing those parameters shown in Figs. 10, 11 with that in Fig. 8. Firstly, both the highest NO_2 mole concentration and production rate is observed at RDR_{NO2}-HO_2 region located at the interface between hot NO-containing combustion products and the cool CH_4/air mixture. Secondly, nearly zero NO_2 is produced in regions featuring with high temperature representing the combustion products of diesel fuel and NG, and regions at relatively low temperature representing the unburned CH_4-air mixture without involving combustion or mixing with combustion products. The volume of NO_2 containing region, NO_2 mole fraction, as well as NO_2 production rate is found to decrease monotonically with the increasing NG substitution ratio.

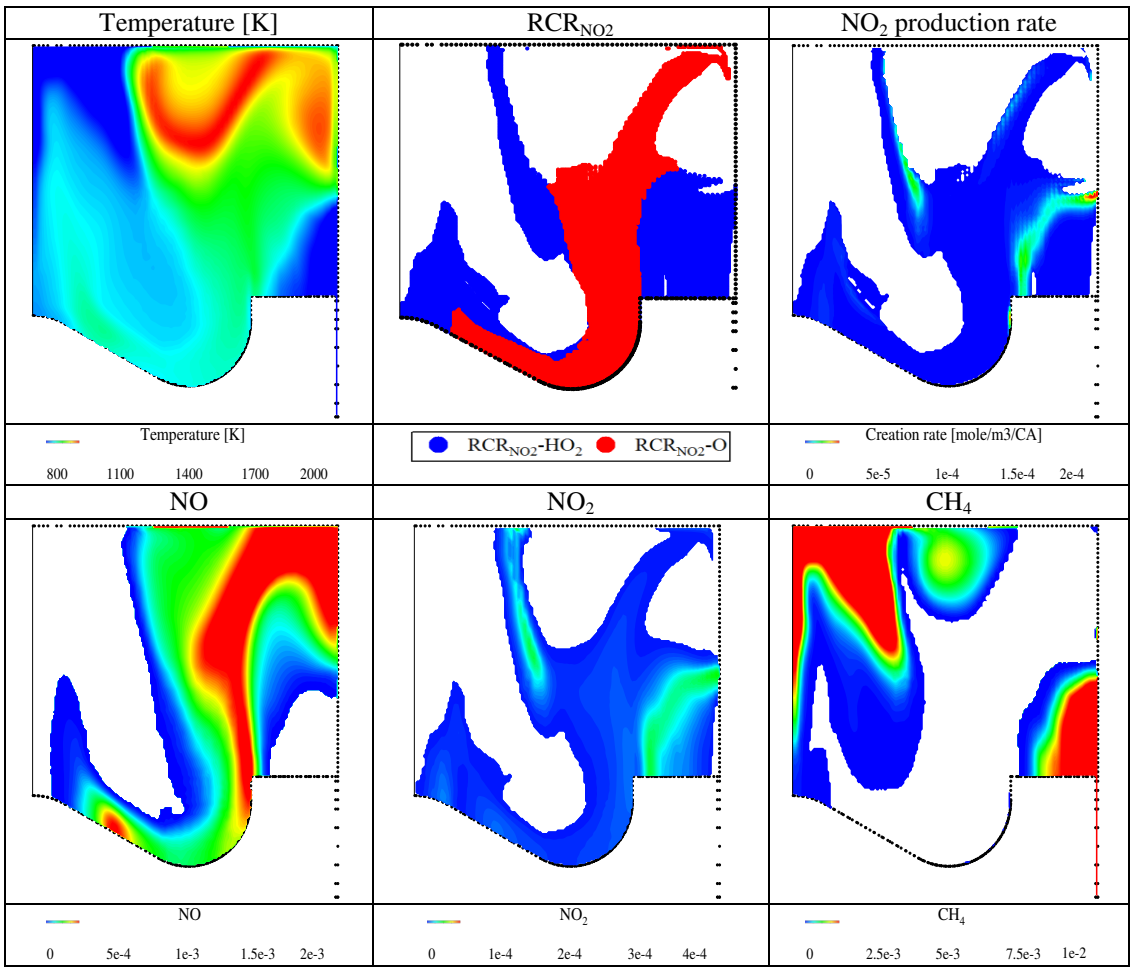

Fig. 10 The temperature, RCR_{NO2} distribution, NO_2 production rate, CH_4, NO, NO_2 molar fraction simulated at Region1, 60 °CA ATDC, 50NG case.

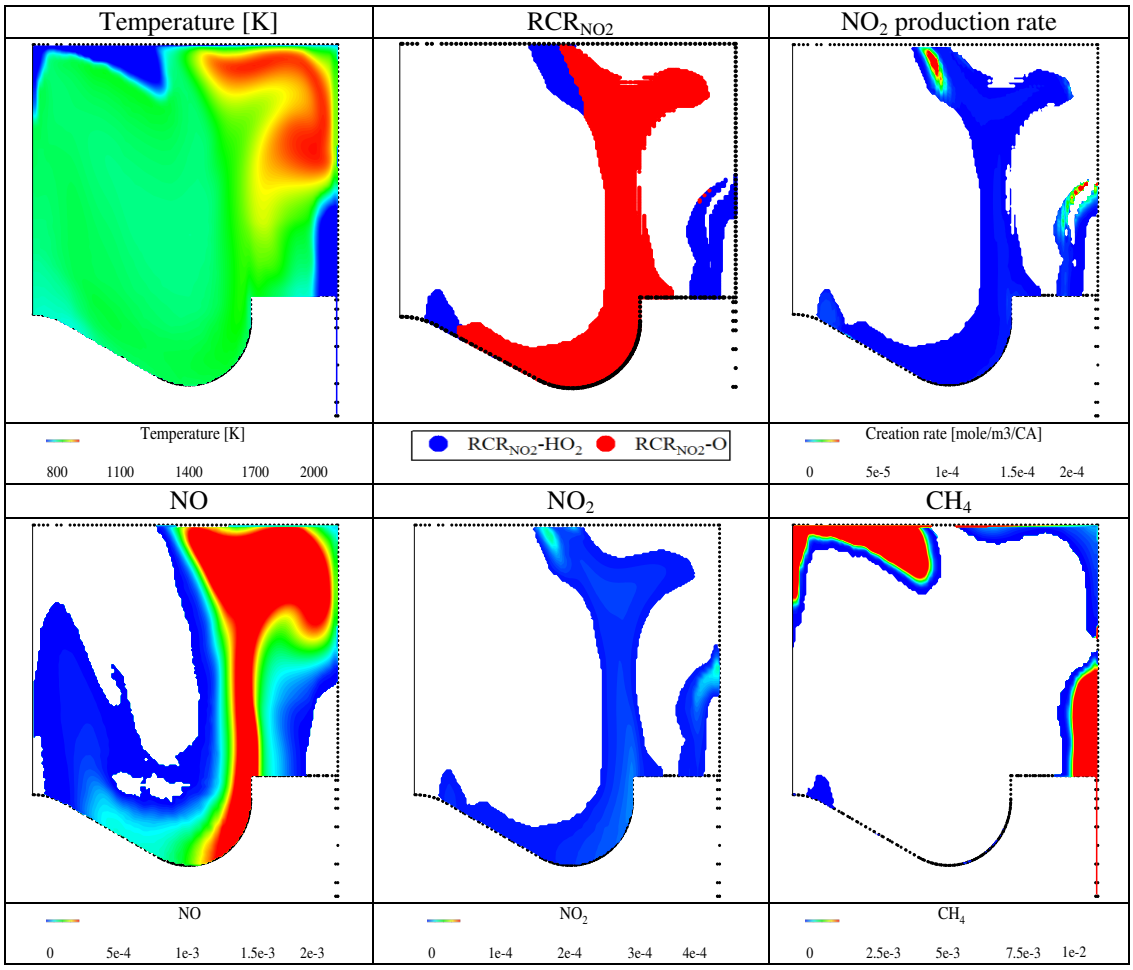

Fig. 11 The temperature, RCR_{NO2} distribution, NO_2 production rate, CH_4, NO, NO_2 molar fraction simulated at Region1, 60 °CA ATDC, 75NG case.

Moreover, as shown in Fig. 12, increasing the substitution ratio from 25NG to 50NG slightly decreased the total volume of the RCR_{NO2}-HO_2 region until about 100 °CA ATDC. The slightly higher RCR_{NO2}-HO_2 region volume was only observed during the late expansion process. However, increasing the substitution ratio from 25NG to 50NG significantly decreased the reaction rate of R1. Therefore, the decreased NO_2 emissions at 50NG when compared with 25NG were due to the decreased reaction rate of R1. Further increasing NG substitution ratio to 75NG decreased the volume of the RCR_{NO2}-HO_2 region, R1 reaction rate, and NO_2 formed in the RCR_{NO2}-HO_2 region. Increasing the substitution ratio decreases the mass of diesel injected into the cylinder, the size of diesel spray plume, and the volume of hot combustion products as the mass of the diesel injected was significantly decreased. At same time, the increased methane concentration at 75NG helps to burn more NG-air mixture presented outside diesel spray than that at lower substitution ratio and decreased the volume of unburned NG-air observed during the late combustion stage and post combustion expansion process. This is due to the burning of more NG-air mixture at higher substitution ratio benefiting from the higher concentration of NG in intake mixture. This is supported by the portion of the unburned methane-air mixture shown in Figure 11 compared to 25NG and

50NG cases shown in Figure 8 and Fig. 10, respectively. These explain the variation of the RCR_{NO2}-HO_2 region observed at 75NG as it is directly associated with the volumes of the hot combustion products and the cool methane-air mixture. Additionally, the variation of the overall reaction rate is not only affected by the volume of the RCR_{NO2}-HO_2 region but also by the local temperature, concentration of methane, and how the combustion products interact with the cool NG-air mixture. Furthermore, according to Arrhenius expression, the reaction rate is sensitive to local temperature. Thus, the factors that affect the local temperature, such as heat release process and changes in thermal capacity (specific heat), also affect the reaction rate of R1 in the RCR_{NO2}-HO_2 region. However, the volume of RCR_{NO2}-HO_2 region monotonically decreased with the increasing NG substitution ratio.

The formation of NO_2 in NG-diesel dual fuel engines is affected by many factors. Among these, the presence of unburned methane especially after the completion of combustion or other species having the potential to produce HO_2 and the NO-containing combustion products, the mixing between the two mixtures during and after the main combustion process, and production of HO_2 during the oxidation process of methane and its reaction with NO previously formed in the hot combustion products are the key factors dominating the formation of NO_2 in NG-diesel dual fuel engines. The control of the formation of NO_2 should focus on the approaches either to minimize or maximize the availability of HO_2 and its reaction with NO when mixed with hot combustion products.

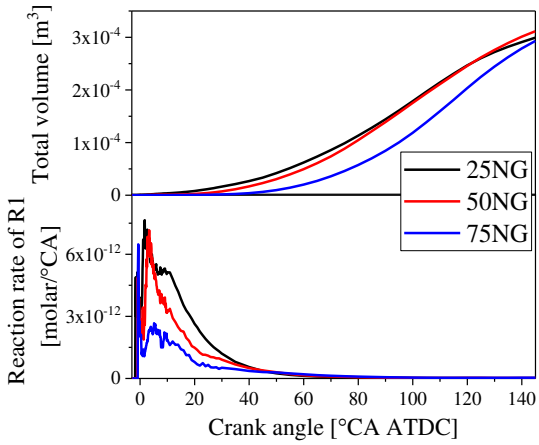

Fig. 12 The volume of the RCR_{NO2}-HO_2 region and average reaction rate of R1 in the RCR_{NO2}-HO_2 region.

Conclusion

This paper investigated the NO_2 formation reaction pathway in a NG-diesel dual fuel engine operating at low loads. The reactions dominating NO_2 formation were revealed by examining the instantaneous ROP of key species calculated using the in-house post process tools with the known temperature, pressure, and concentration of key species simulated using CFD. The formation reaction pathway of key species such as O and HO_2 dominating NO_2 formation has been derived. The impacts of temperature on the reaction rate constant of key reactions dominating the chemical reactions in the RCR_{NO2}-O and RCR_{NO2}-HO_2 regions were investigated. All of the following conclusions may only be true at the operating conditions investigated and for the engine hardware used.

Based on the data presented in this research, these conclusions can be drawn at the investigated conditions:

1) The NO_2 in a NG-diesel dual fuel engine can be formed in the RCR_{NO2}-O and RCR_{NO2}-HO_2 regions. The RCR_{NO2}-O region represents the formation of NO_2 at high-temperature combustion products during the main combustion stage of diesel fuel. The RCR_{NO2}-HO_2 region represents the interface between the hot NO-containing combustion products and the cool methane-containing unburned methane-air mixture. The increased NO_2 emissions from dual fuel engines are mainly formed in the RCR_{NO2}-HO_2 region.

2) The HO_2 radical required for NO-NO_2 conversion in the RCR_{NO2}-HO_2 region is produced by the reaction pathway: CH_4->CH_3->CH_2O->HCO->HO_2. The presence of the RCR_{NO2}-HO_2 region contributes to the significantly increased NO_2 emissions from a NG-diesel dual fuel engine compared to a traditional diesel engine. The unburned CH_4/air that survives the main combustion stage provides the methane source for production of HO_2 leading to the formation of more NO_2 in NG-diesel dual fuel engines than traditional diesel engines.

3) The O radical required for NO-NO_2 conversion in the RCR_{NO2}-O region is produced by the reaction pathway: HCO->H->O, through reaction R17 and R18 with HCO produced during the oxidation process of n-Heptane noted as C_7H_{15}->CH_2O->HCO->H->O->NO_2. The examination of the reaction rate constant reveals that the key factor causing R17 and R18 to dominate HCO and H radical consumption is the high temperature. Therefore, the RCR_{NO2}-O region is featured with high temperature and rich O_2. Meanwhile, the high temperature can promote the destruction of NO_2 to NO by R3 and R4. As a result, the NO_2 concentration in the RCR_{NO2}-O region is lower than that in the RCR_{NO2}-HO_2 region. In addition, the NO_2 eventually emitted from dual fuel engines is mainly formed in the RCR_{NO2}-HO_2 region.

4) The emission of NO_2 in a NG-diesel dual fuel engine is determined by total volume of RCR_{NO2}-HO_2 region and R1 reaction rate in the RCR_{NO2}-HO_2 region. Compared with the 25NG case, the 50NG case has similar RCR_{NO2}-HO_2 region volume but significantly lower R1 reaction rate due to combined effect of various factors such as local temperature, CH_4 concentration, and interaction between hot NO-containing combustion products and cool CH_4/air mixture. The total volume and R1 reaction rate of the RCR_{NO2}-HO_2 region observed in the 50NG and 75NG cases are both lower than the 25NG case.

Acknowledgement

The support of Convergent Science toward this research is gratefully appreciated. The author acknowledges the funding support provided by Natural Resources Canada through the PERD Energy End Use (project 3B03.003) and National Research Council Canada through the internal Bioenergy Program.

Reference

[1] Boezen, H. M., van der Zee, S. C., Postma, D. S., Vonk, J. M., Gerritsen, J., Hoek, G., & Schouten, J. P. Effects of ambient air pollution on upper and lower respiratory symptoms and peak expiratory flow in children. The Lancet, 353(9156), (1999) 874-878.

[2] Karim G A. Dual-fuel diesel engines [M]. CRC Press, 2015.

[3] Liu, S., Li, H., Gatts, T., Liew, C., Wayne, S., Thompson, G., & Nuszkowski, J. An investigation of NO2 emissions from a heavy-duty diesel engine fumigated with H2 and natural gas. Combustion Science and Technology, 184(12), (2012) 2008-2035.

[4] Liu, S., Li, H., Liew, C., Gatts, T., Wayne, S., Shade, B., & Clark, N. An experimental investigation of NO_2 emission characteristics of a heavy-duty H 2-diesel dual fuel engine. International journal of hydrogen energy, 36(18), (2011) 12015-12024.

[5] Lilik, G.K., Hydrogen assisted diesel combustion. MS Thesis. Department of Energy and Geo-Environmental Engineering, The Pennsylvania State University, University Park, PA; 2008

[6] Lilik, G. K., Zhang, H., Herreros, J. M., Haworth, D. C., & Boehman, A. L. Hydrogen assisted diesel combustion. International journal of hydrogen energy, 35(9), (2010) 4382-4398.

[7] Bika, A. S., Franklin, L. M., & Kittelson, D. B. Emissions effects of hydrogen as a supplemental fuel with diesel and biodiesel. SAE International Journal of Fuels and Lubricants, (2008), 1(2008-01-0648), 283-292.

[8] Zhou, J. H., Cheung, C. S., & Leung, C. W. Combustion and emission of a compression ignition engine fueled with diesel and hydrogen-methane mixture. World Academy of Science, Engineering and Technology, International Journal of Mechanical, Aerospace, Industrial, Mechatronic and Manufacturing Engineering, 7(8), (2013) 1653-1658.

[9] Nelson, P. F., & Haynes, B. S. "Hydrocarbon-NOx interactions at low temperatures—1. Conversion of NO to NO_2 promoted by propane and the formation of HNCO." Symp. (Int.) Combust. 25(1) (1994) 1003-1010.

[10] Hori, M., Matsunaga, N, Marinov, N., Pitz, W., and Westbrook, C. "An experimental and kinetic calculation of the promotion effect of hydrocarbons on the NO-NO_2 conversion in a flow reactor." Symp. (Int.) Combust. 27(1) (1998) 389-396.

[11] Mueller, M. A., Yetter, R. A., & Dryer, F. L. Mueller. "Flow reactor studies and kinetic modeling of the H_2/O_2/NOx and CO/$H_2O/O_2/NO_x$ reactions." International Journal of Chemical Kinetics, 31(10), 1999, 705-724.

[12] Kyne, A. G., Pourkashanian, M., Wilson, C. W., & Williams, A. Kyne. "Modelling NO-NO_2 Conversion in Counter-Flow Diffusion Flames." ASME Turbo Expo 2003, collocated with the 2003 International Joint Power Generation Conference. American Society of Mechanical Engineers, 2003: 19-26.

[13] Richards, K. J., Senecal, P. K., and Pomraning, E., CONVERGE (v2.3), Convergent Science, Madison, WI.

[14] Ra, Y., Reitz, R D. A reduced chemical kinetic model for IC engine combustion simulations with primary reference fuels [J]. Combustion and Flame, 155(4) (2008) 713-738.

[15] Li, Y., Guo, H, Li, H. "Evaluation of Kinetics Process in CFD Model and Its Application in Ignition Process Analysis of a Natural Gas-Diesel Dual Fuel Engine," SAE Technical Paper 2017-01-0554.

[16] Design, R. CHEMKIN Theory Manual [J]. San Diego, CA, 2007.

[17] Guo, H., Neill, W.S., and Liko, B. "An Experimental investigation on the combustion and emissions performance of a natural gas–diesel dual fuel engine at low and medium loads." ASME 2015 Internal Combustion Engine Division Fall Technical Conference, Houston, TX, Nov. 8 -11, 2015.

[18] Smith, G.P., Golden, D.M., Frenklach, et al: <http://www.me.berkeley.edu/gri_Mech/.GRI-mech3.0,2005>.

[19] Li, Y., Li, H., Guo, H., Li, Y., and Yao, M. A numerical investigation on methane combustion and emissions from a natural gas-diesel dual fuel engine using CFD model. Applied Energy, 205 (2017) 153-162.

[20] Heywood, J.B., Internal Combustion Engine Fundamental, 1988, McGraw-Hill, Inc

[21] Turns, S., An introduction to combustion: concepts and applications, 2012, McGraw-Hill, Inc